Transient response of immobilized enzyme reactors - the effects of reactor type and shape of core-shell bio-catalytic pellets

Young-Sang Cho†

Department of Chemical Engineering and Biotechnology, Tech University of Korea,
237 Sangdaehak-ro, Siheung-si, Gyeonggi-do 15073, Korea

Abstract−Transient responses of immobilized enzyme reactors were obtained by solving coupled governing equations for core-shell catalytic pellets. The morphology of the pellets was assumed as sphere, cylinder, and slab-type particles having inert cores. Nonlinear reaction-diffusion equations of batch-mode reaction systems were solved by finite element method using commercial software, COMSOL Multiphysics, to investigate the effect of adjustable parameters such as thickness of inert core, *Biot* number, and the amount of pellets as well as reaction parameters of Michaelis-Menten kinetics. Modeling of CSTR was also carried out and the results were compared with the transient response of batch reactor by adjusting retention time during numerical calculations, reflecting deactivation of enzyme as time-dependent rate constant. For both types of reactors, spherical pellets were the most advantageous for reduction of reactant concentration with relatively smaller effect of the thickness of inert core, compared to other types of pellets. Additionally, a number of connected CSTRs were assumed for approximate analysis of fixed bed reactor, of which the behavior became close to a simple CSTR with increasing axial dispersion.

Keywords: Immobilized Enzyme Reactor, Core-shell Pellets, Enzyme Inactivation, Fixed Bed Reactors

INTRODUCTION

Immobilized enzymes have been intensively studied to develop effective schemes for chemical binding of enzymes on supports and preparation of functional supporting materials for coating of enzymes to produce useful chemicals or biofuels in pharmaceutical and food industries as well as agricultural engineering [1-4]. Various kinds of reactors containing immobilized enzymes have been designed and adopted to promote the rate of biochemical reactions and scale-up of reaction systems [5-8]. Recently, core-shell particles with magnetic cores have been synthesized as supporting materials of immobilized enzymes for separation of the biological catalyst from reaction medium under a magnetic field [9,10]. Droplet-assisted microfluidic devices have been studied for preparation of immobilized enzyme pellets in a continuous manner [11]. Temperature-sensitive reversible release and loading of enzymes have been also studied to synthesize controllable immobilized enzymes [12]. In reaction engineering, mathematical modeling of immobilized enzyme reactors has been also performed for analysis of the reaction system with the aid of numerical scheme by computation, thus enabling the prediction of reaction conversion or effectiveness factor [13-17].

Compared to free enzymes, it is advantageous to use immobilized enzymes for biological reactions, because they can be used as more stable bio-catalytic materials due to easy recovery and control in reaction systems [18]. Though fruitful results on mathematical modeling of immobilized-enzyme reactor have been obtained by Lin and Wei, they assumed enzyme-immobilized pellets with spherical morphology without inert core [19]. However, this assumption is not adequate for a real situation, because enzyme immobilization is accomplished by binding enzymes onto supporting particles like alginate gel having no enzymatic activity, implying that the uniform distribution of enzymes in immobilized enzyme pellets cannot be guaranteed in a real situation [20]. Moreover, supporting materials for immobilization have been developed as core-shell particles, which possess non-uniform composition and structures. Thus, it is essential to model the pellets of biological catalysts as core-shell particles with inert core, though mathematical treatment becomes more complicated. The difficulties for solving governing equations for inert-core structures as well as non-linear reaction kinetics of biological reactions can be resolved by using a useful numerical scheme like the finite element method.

Though fixed beds are widely used as immobilized-enzyme reactors for industrial production in food and pharmaceutical industries due to long retention time, batch-mode reactors are also valuable for prediction of reaction parameters of proper kinetics model [21]. As a continuous reactor, CSTRs (continuously stirred tank reactors) are also convenient, because the temperature and concentration of reactant can be controlled uniformly using proper mixing apparatuses [22,23]. However, there exists some drawback in the batch reactor and CSTR, because the suspended immobilized-enzyme catalysts can be lost in the outlet stream. Thus, modeling of fixed bed immobilized enzyme reactors is still necessary by assuming core-shell pellets. During modeling, enzyme deactivation can be also considered for exact prediction of reactor performance, because catalytic activity of enzymes decreases with increasing reac-

†To whom correspondence should be addressed.
E-mail: yscho78@kpu.ac.kr, yscho78@tukorea.ac.kr

tion time [19,24].

In the present study, the immobilized enzyme reactors were modelled by solving coupled governing equations of solid and fluid phases simultaneously. Non-linear reaction kinetics like Michaelis-Menten kinetics was reflected in the mathematical equations by considering time-dependent rate constant for enzyme inactivation, and numerical solutions of the resulting differential equations were obtained by finite element method. The factors affecting the performance or reaction conversion of batch-mode reactors were investigated by adjusting the parameters of reaction kinetics, *Biot* number, and the amount of catalyst loading. For various morphologies of catalytic pellets, such as sphere, cylinder, slab, as well as their core-shell structures, the effects of reaction parameters were studied systematically from abundant calculation results. The effects of retention time and the size of catalytic pellets were also studied for prediction of the performance of CSTRs containing immobilized-enzyme pellets with different shapes. As an approximation of fixed bed reactor, the cascade connection of sufficient number of CSTRs was assumed with interchanging streams of reactant and product between the connected reactors, and the effect of axial dispersion was investigated to avoid the complicated mathematical treatment of the fixed bed reactor.

COMPUTATION AND MODELING METHODS

For three kinds of geometries of bio-catalytic pellets described schematically in Fig. 1(a) to (c), uni-axial diffusion was assumed during mathematical modeling. For instance, mass transport in polar and azimuthal angle was ignored in spherical pellets, whereas diffusion along azimuthal angle and height direction was not considered in cylindrical particles. In slab-type pellets, uniaxial diffusion along perpendicular direction to slab-surface was only considered to derive reaction-diffusion equations.

At first, batch-mode immobilized enzyme reactor described schematically in Fig. 1(d) were considered for modeling to derive governing equations about reactant concentration inside core-shell pellets, c_p and the concentration in bulk fluid phase, C_b, assuming the following enzymatic reaction with one substrate.

$$S + E \longleftrightarrow E \cdot S \rightarrow E + P \tag{1}$$

Though Michaelis-Menten kinetics was assumed for modeling, the mathematical approaches in this study can be extended to more complicated kinetics of biological reactions with the aid of the development of numerical analysis and computing apparatuses. Additionally, reactants of more than two kinds (bisubstrate) can be also considered for governing equations inside the particles [25, 26]. Because the activity of enzymes decays as a function of time, enzyme inactivation was reflected in the rate constant, k_0, as first-order deactivation with reaction time, as presented in the following equations for batch reactors.

$$\frac{\partial c_p}{\partial t} = \frac{D_e}{r^z}\frac{\partial}{\partial r}\left(r^z\frac{\partial c_p}{\partial r}\right) - \frac{k_0\exp(-k_E t)E_0 c_p}{c_p + k_m}$$

$$\text{and } V\frac{dC_b}{dt} = -\frac{z+1}{R}\frac{m_p}{\rho_p}D_e\left(\frac{\partial c_p}{\partial r}\right)_{r=R} \tag{2}$$

subject to boundary conditions such as $(\partial c_p/\partial r)_{r=x'R}=0$ and $D_e(\partial c_p/\partial r)_{r=R}=k_f[C_b(t)-c_p(R, t)]$ and initial conditions such as $c_p(r, 0)=0$ and $C_b(0)=C_0$

Here, V is the volume of batch reactor, m_p and ρ_p stand for mass and density of the pellets with immobilized enzyme, respectively. E is the concentration of enzyme, while r and R are radial distance from the center of the pellets and the radius of the pellets, respectively. Because enzyme deactivation was reflected using deactivation constant, k_E, E can be represented as $E_0\cdot\exp(-k_E t)$ using the first order kinetics. D_e is effective diffusivity of reactant inside the
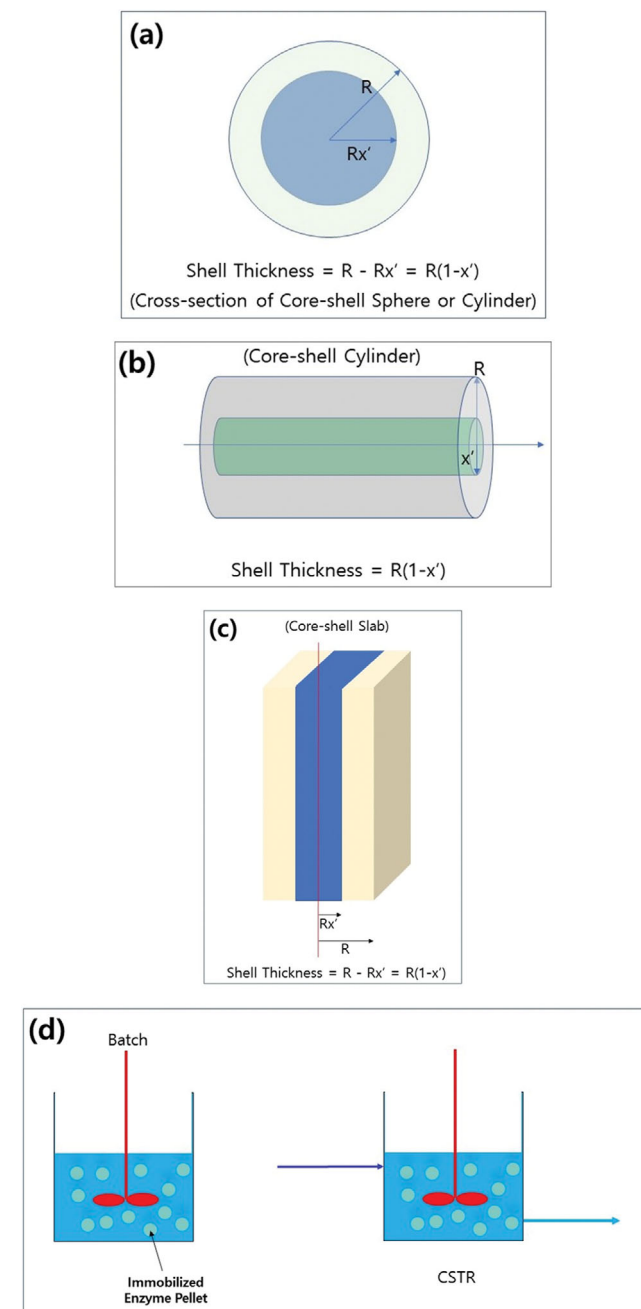

Fig. 1. Schematic of enzyme-immobilized pellets with (a) spherical, (b) cylindrical, and (c) slab-type morphologies. (d) Schematic of enzyme-immobilized reactors such as batch and CSTR.

pellets. k_e is defined as deactivation constant of enzyme reaction, whereas k_m stands for the Michaelis-Menten kinetics. For modeling of the catalytic pellets with different geometries, z is defined as 2, 1, and 0 for sphere, cylinder, and slab, respectively. In the boundary condition, x'R and k_f are the radius of inert core and mass transfer coefficient, respectively. The above equations can be non-dimensionalized in the following manner by defining dimensionless reactant concentration y_p and y_b inside particle and bulk phase, respectively.

$$\frac{\partial y_p}{\partial \tau} = \frac{1}{x^z}\frac{\partial}{\partial x}\left(x^z\frac{\partial y_p}{\partial x}\right) - \frac{\phi^2 \exp(-K_e\tau)y_p}{y_p + K_m}$$

$$\text{and } \frac{dy_b}{d\tau} = -(z+1)\alpha\left(\frac{\partial y_p}{\partial x}\right)_{x=1} \tag{3}$$

subject to boundary conditions such as $(\partial y_p/\partial r)_{x=x'}=0$ and $(\partial y_p/\partial x)_{x=1}=Bi[y_b(\tau)-y_p(1, \tau)]$ and initial conditions such as $y_p(x, 0)=0$ and $y_b(0)=1$

Here, α denotes the amount of catalyst loading, $m_p/(\rho_p V)$; Φ^2 is defined as square of Thiele modulus, $k_0 R^2 E_0/(S_0 D_e)$. Dimensionless reaction time, τ is defined as tD_e/R^2, while K_e is $k_e R^2/D_e$; dimensionless distance from the center of the pellets, x, is defined as r/R. In boundary condition, Bi stands for Biot number, $k_f R/D_e$. Another reaction parameter, k_e is non-dimensionalized as K_e by defining k_e/S_0. In this study, the above nonlinear coupled differential equations were solved by finite element method using COMSOL Multiphysics software by defining extremely fine mesh.

RESULTS AND DISCUSSION

1. Modeling of Batch-mode Enzyme-immobilized Reactor

The transient response of batch enzyme-immobilized reactor was predicted assuming core-shell slab-type pellets suspended in the reactor. As the thickness of inert core, x', increases, the steady-state concentration of substrate increases due to decrease of active volume of the pellets loaded with enzymes, as presented in Fig. 2(a). Detailed reaction conditions are summarized in Table 1. The conversion of reactant can be enhanced by increasing the rate
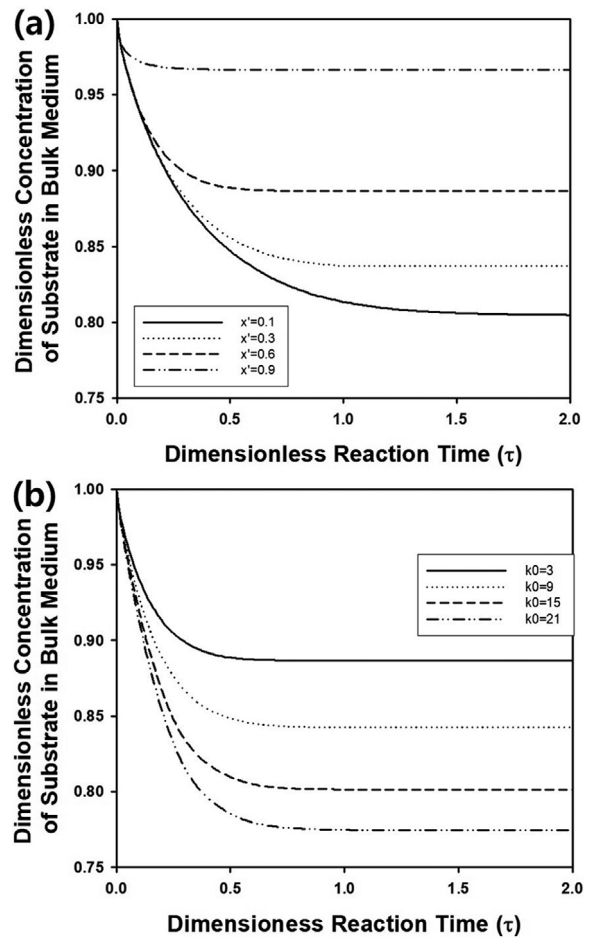

Fig. 2. (a) Change of dimensionless concentration of reactant in bulk medium as a function of reaction time in batch reactor containing core-shell slab-type pellets with various values of inert-core thickness, x'. k_0, α, Φ, K_e, K_m, and *Bi* were fixed as 3, 0.2, 3.5355, 10, 0.5, and 10, respectively. (b) Change of dimensionless concentration of reactant in bulk medium as a function of reaction time in batch reactor containing core-shell slab-type pellets for various values of k_0. x', α, K_e, K_m, and *Bi* were fixed as 0.6, 0.2, 10, 0.5, and 10, respectively.

Table 1. Parameters for calculation of batch immobilized enzyme reactor. VAR means 'variable'

|	k_0	α	K_e	K_m	Bi	x'	τ	Reaction temperature	Shape of pellets
Fig. 2(a)	3	0.2	10	0.5	10	VAR	-	-	Core-shell slab
Fig. 2(b)	VAR	0.2	10	0.5	10	0.6	-	-	Core-shell slab
Fig. 3(a)	21	0.2	10	VAR	10	0.6	-	-	Core-shell cylinder
Fig. 3(b)	21	0.2	VAR	0.5	10	0.6	-	-	Core-shell cylinder
Fig. 3(c)	VAR	0.2	1	0.5	10	0.3	-	VAR	Core-shell cylinder
Fig. 4(a)	21	VAR	5	2	10	0.6	-	-	Core-shell sphere
Fig. 4(b)	21	0.4	5	2	VAR	0.6	-	-	Core-shell sphere
Fig. 4(c)	21	0.4	5	2	10	0.6	VAR	-	Core-shell sphere
Fig. 4(d)	21	0.4	5	2	10	VAR	0.05	-	Core-shell sphere
Fig. 5(a)	21	0.4	5	2	10	0.01	-	-	VAR
Fig. 5(b)	21	0.4	5	2	10	0.01	∞	-	VAR
Fig. 5(c)	21	0.4	5	2	10	VAR	∞	-	VAR
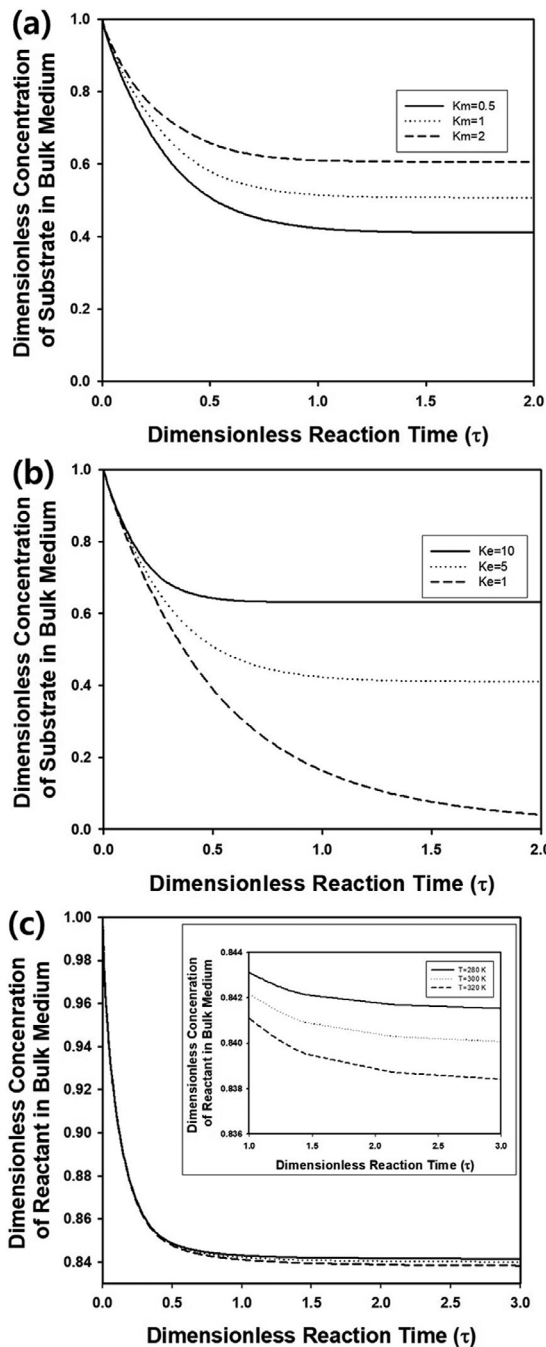
Fig. 3. (a) Change of dimensionless concentration of reactant in bulk medium as a function of reaction time in batch reactor containing core-shell cylindrical pellets for various values of K_m. x', k_0, α, K_e, and Bi were fixed as 0.6, 21, 0.2, 10, and 10, respectively. (b) Change of dimensionless concentration of reactant in bulk medium as a function of reaction time in batch reactor containing core-shell cylindrical pellets for various values of K_e. x', k_0, α, K_m, and Bi were fixed as 0.6, 21, 0.2, 0.5, and 10, respectively. (c) Change of dimensionless concentration of reactant in bulk medium as a function of reaction time in batch reactor containing core-shell cylindrical pellets for various values of reaction temperature. x', α, K_m, K_e, and Bi were fixed as 0.3, 0.2, 0.5, 1, and 10, respectively. Activation energy was assumed as 10,000 J/(molK). Inset figure contains magnified graph from $\tau=1$ to 3.

constant, k_0, due to increased removal rate of the reactant, as shown in Fig. 2(b). Though slab-type pellets are not common in industry, the performance of an enzyme-immobilized reactor containing slab-type catalyst can be compared with the results from other types of pellets such as cylinders and spheres, as discussed in this study.

For practical applications, cylindrical pellet is more common geometry compared to slab-type pellet. Thus, the effect of reaction parameter, K_m, was investigated by calculating $y_b(\tau)$ in batch reactor containing cylindrical pellets for three different values of K_m, such as 1, 5, and 10, as presented in Fig. 3(a). As K_e increased, the saturation rate of the bulk concentration became faster and the steady-state concentration in bulk medium increased to higher value, because reaction rate decreased with increasing value of K_m. In Fig. 3(b), the effect of enzyme deactivation was also studied by adjusting deactivation parameter, K_e, from 1 to 10. As K_e decreased, steady-state concentration in bulk medium became smaller, because the inactivation rate of immobilized enzymes became slower. The temperature (T) dependence of rate constant can be also represented as Arrhenius type, $k_0=k_{0,p} \cdot \exp\{-E_a/(RT)\}$, assuming uniform mixing inside the batch reactor. As T increased from 280 to 320 K, the reaction conversion at steady state increased slightly, indicating that the performance of batch reactor can be enhanced by increasing T, as presented in Fig. 3(c).

Since spherical pellets are the most common morphologies in catalysis, the effect of enzyme loading, α, was studied by calculating $y_b(\tau)$ for three different values of α, such as 0.2, 0.3, and 0.4. As displayed in Fig. 4(a), steady-state concentration of bulk medium decreased with increasing value of α, because active sites for enzyme catalysis reaction increased with increasing amount of the enzyme-immobilized pellets. The effect of $Biot$ number was also studied for spherical pellets by changing Bi from 0.1 to 10, and the results are plotted in Fig. 4(b). In this model, the resistance over the mass transfer of reactant can be considered for two different regions. During modeling, the resistance of intra-particle diffusion and convective transfer in the film surrounding the pellets can be considered by defining $Biot$ number. Because the mass transfer resistance near the film decreases with increasing Bi, the bulk concentration of reactant in batch reactor decreased more rapidly and the concentration at stationary state decreased due to enhanced mass transfer rate of reacting species to the pellets from bulk medium. In a batch-mode reactor, Bi can be increased by increasing agitation speed of impeller, implying that sufficient reaction conversion can be expected by controlling mixing quality of the reaction system [27]. In Fig. 4(c), the profiles of reactant concentration inside the core-shell spherical pellets are predicted from $y_p(x, \tau)$ for various values of reaction time. Because there was no reactant inside the pellets in the initial stage of reaction, the concentration profile increased with increasing value of τ. For all reaction times, the predicted value of the reactant concentration increased with increasing x, because the direction of diffusional transport of reacting species through the pellets is from the particle surface to inner region of the pellets. However, the concentration profile became uniform with increasing τ, indicating that diffusion rate decreases as reaction proceeds. In Fig. 4(d), the concentration profiles inside core-shell pellets were predicted for different values of inert core thick-
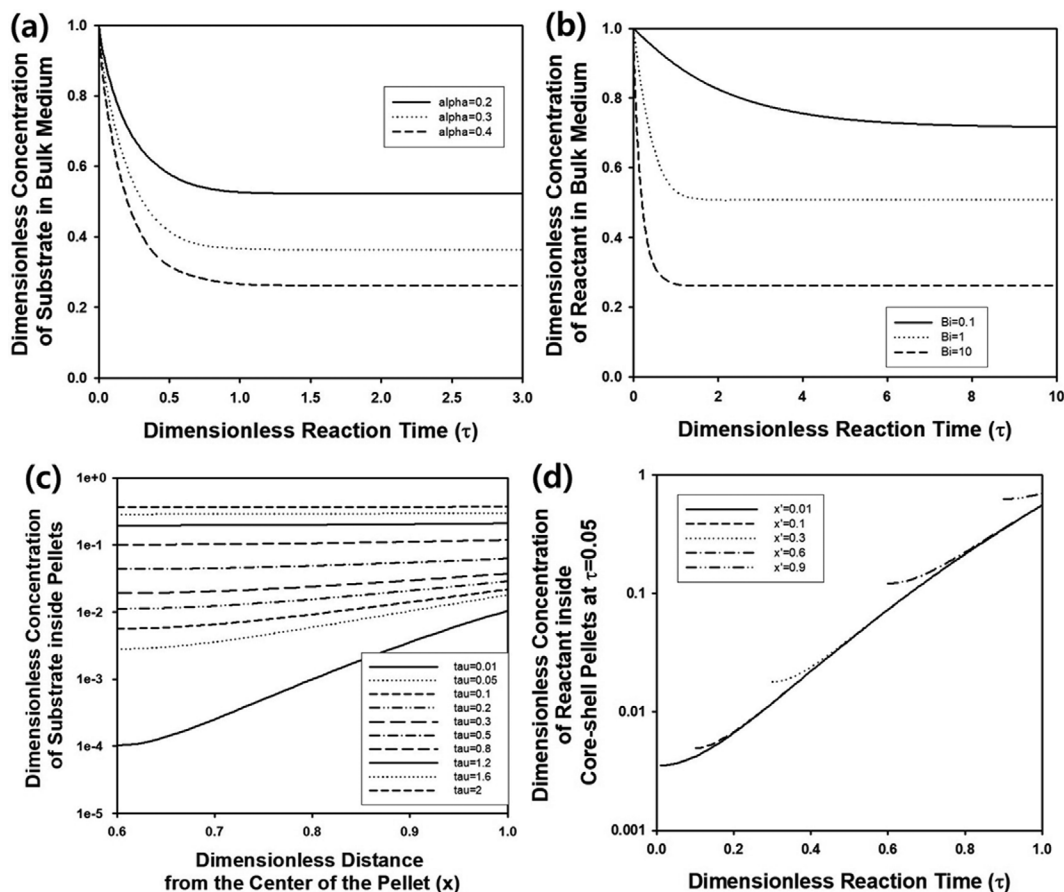
Fig. 4. (a) Change of dimensionless concentration of reactant in bulk medium as a function of reaction time in batch reactor containing core-shell spherical pellets for various values of α. x', k_0, K_e, K_m, and Bi were fixed as 0.6, 21, 5, 2, and 10, respectively. (b) Change of dimensionless concentration of reactant in bulk medium as a function of reaction time in batch reactor containing core-shell spherical pellets for various values of Bi. x', α, k_0, K_e, and K_m were fixed as 0.6, 0.4, 21, 5, and 2, respectively. (c) Time-lapse profile of reactant concentration inside core-shell spherical pellet for various values of τ from 0.01 to 2. x', α, k_0, K_e, and K_m, Bi were fixed as 0.6, 0.4, 21, 5, 2, and 10, respectively. (d) Concentration profile of reactant inside core-shell spherical pellet for various values of x' at τ=0.05. α, k_0, K_e, K_m, and Bi were fixed as 0.4, 21, 5, 2, and 10, respectively.

ness at τ=0.05. For all calculation results, the concentration increased as x increased, which confirms the inward diffusional flux of reactant. However, the overall concentration increased with increasing value of x', because there is no contribution of inert core to reaction conversion.

To compare the reactor performance of batch reactor containing three different types of catalytic pellets, transient concentrations were calculated under the same reaction conditions by fixing α, K_e, K_m, k_0, and Bi as 0.4, 5, 2, 21, and 10, respectively. The pellets were assumed as core-shell particles with very thin inert core thickness, x' as 0.01. As presented in Fig. 5(a), the best performance with the lowest steady-state concentration in bulk fluid phase was predicted from the batch reactor containing spherical pellets, compared to other shapes of the catalytic particles, because interfacial area of spheres per unit volume of reactor is more larger than that of cylinder and slab-type particles. In Fig. 5(a), the transient responses of the average concentration of reactant inside the pellets were also

plotted by calculating $\overline{y_p}(\tau) = \dfrac{z+1}{1-x^{z+1}} \displaystyle\int_{x=x'}^{1} x^z y_p(x, \tau) dx$ with z=2, 1,

and 0 for sphere, cylinder, and slab-type pellets, respectively. Regardless of the shape of the pellets, the average intra-particle concentration increased from 0 to steady-state value, which is the same as the concentration in bulk fluid phase. Because the mass transfer rate from the bulk phase to the pellets is proportional to the difference between y_b and $\overline{y_p}(\tau)$, steady-state concentration can be defined in batch reactor containing enzyme-immobilized pellets with time-dependent inactivation. However, the steady-state concentration is simply 0 in the batch catalytic reactor, assuming irreversible first-order reaction. In Fig. 5(b), the effect of the shape of the catalytic pellets was studied by plotting the concentration of reactant at steady state, y_∞ as a function of the thickness of inert core, x', by increasing α as 0.4. y_∞ decreased with decreasing value of x' due to the increase of active volume of catalytic pellets, while reaction conversion, X, increased with decreasing value of x', because of the definition of X as $1-y_\infty$, as presented in Fig. 5(c). When x' was kept as the same value, the reaction conversion of batch reactor increased in the order of sphere>cylinder>slab, because the surface area of the pellets per unit volume of the reactor increases in the order of
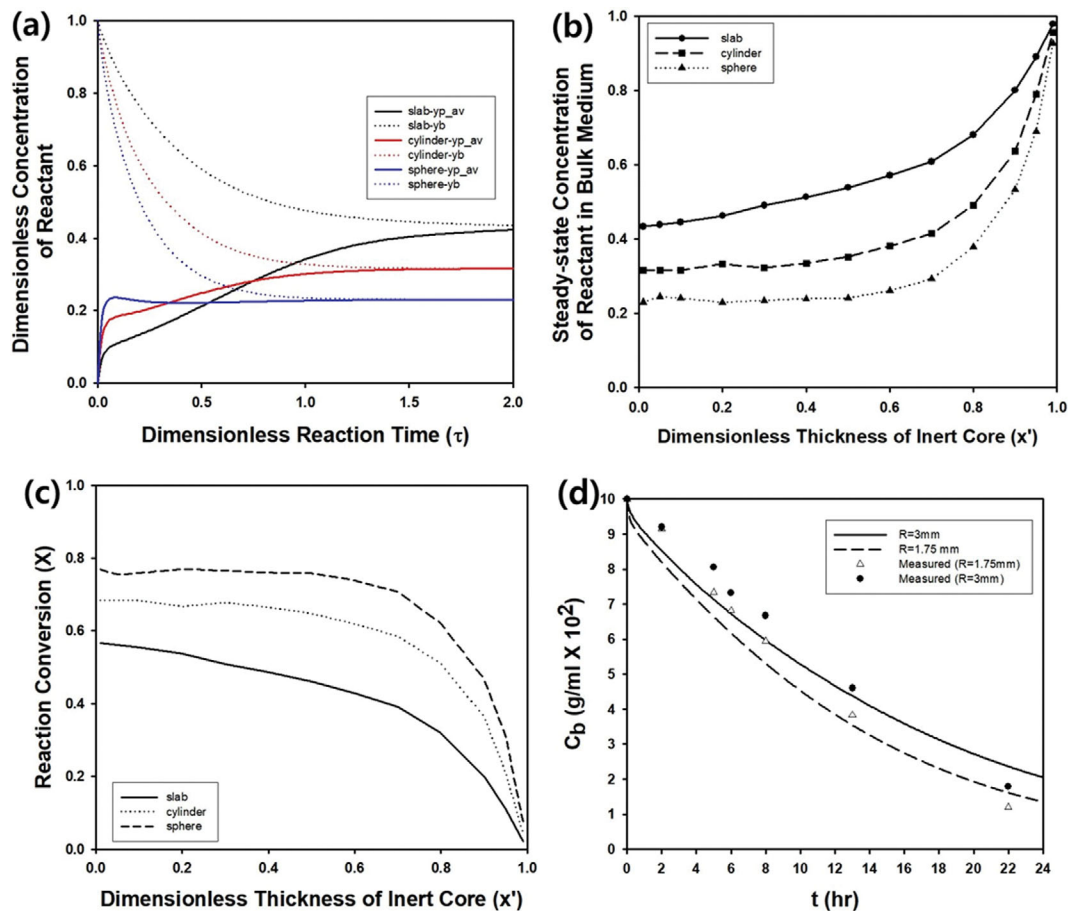
Fig. 5. (a) Change of dimensionless bulk concentration of reactant in bulk liquid and average intra-particle concentration as a function of reaction time in batch reactor containing three different types of immobilized enzyme pellets. x′, α, k_0, K_e, K_m, and *Bi* were fixed as 0.01, 0.4, 21, 5, 2, and 10, respectively. The data in black, red, and blue color indicate the calculation results from slab, cylinder, and spherical pellets, respectively. (b) Change of steady-state concentration in bulk fluid phase and (c) the reaction conversion in batch reactor containing core-shell spherical pellets at steady state as a function of x′. α, k_0, K_e, K_m, and Bi were fixed as 0.4, 21, 5, 2, and 10, respectively. (d) Change of concentration of sucrose in liquid as a function of reaction time. x′, D_e, V, C_{b0}, k_0E_0, k_m, and α were fixed as 0, $4{\times}10^{-10}$ m^2/s, 0.1 L, 0.1 g/ml, 0.256 g/(ml·hr), 0.165 g/ml, and 0.08, respectively, while the values of R chosen as 0.3 and 0.175 cm.

sphere>cylinder>slab. In addition to simulation, the previous experimental data by other research group were compared with simulation results of in the study.

The robustness of modeling and simulation in this study was confirmed by comparing the calculation results and published experimental data. In Fig. 5(a), data points indicate the concentration of sucrose as a function of reaction time in a batch reactor containing calcium alginate beads with immobilized *S. cerevisiae* [28]. Mehmetoglu measured parameters of Michaelis-Menten kinetics of the biochemical reaction of sucrose using immobilized enzymes as well as diffusion coefficient of sucrose inside the alginate beads. Because the measured values of diffusivity ranged from 4.0 to $4.1{\times}10^{-10}$ m^2/s for alginate bead with radius of 0.3 or 0.175 cm, respectively, $4{\times}10^{-10}$ m^2/s was adopted for convenience regardless of the bead size for simulation. Using the reaction parameters and conditions such as V and C_{b0} as 0.1 L and 0.1 g/ml, respectively, numerical solutions were obtained using COMSOL for two different values of R such as 0.3 and 0.175 cm. Because alginate solution is usually mixed with aqueous solution of enzymes or cells

before solidification, uniform distribution of proteins inside the beads was assumed for calculation by setting x′ as 0. Though detailed conditions for estimation of *Biot* number were not included in the previous research by Mehmetoglu, a sufficiently large value like 50 was assumed as *Bi*. As presented in Fig. 5(d), the overall trend of simulation results and experimental data coincide with each other, though underestimation of the reactant concentration by simulation appeared in the initial stage of reaction, whereas the concentration was predicted as slightly larger value than experimental data as the reaction conversion increased to about 0.9. This can be interpreted as the imperfection of modeling assumptions or unexpected behavior of cells attached to the beads.

2. Modeling of Immobilized Enzyme Reaction System as CSTR

In CSTR, the prediction of reactant concentration inside particles and bulk medium can be carried out by solving the following governing equations as non-dimensional forms.

$$\frac{\partial y_p}{\partial \tau} = \frac{1}{x^z}\frac{\partial}{\partial x}\left(x^z\frac{\partial y_p}{\partial x}\right) - \frac{\phi^2 \exp(-K_e\tau)y_p}{y_p + K_m}$$

and $\sigma\dfrac{dy_b}{d\tau}=y_{in}(\tau)-y_b-(z+1)\dfrac{\beta}{\phi^2}\left(\dfrac{\partial y_p}{\partial x}\right)_{x=1}$ (4)

subject to boundary conditions such as $(\partial y_p/\partial r)_{x=x'}=0$ and $(\partial y_p/\partial x)_{x=1}=Bi[y_b(\tau)-y_p(1,\ \tau)]$ and initial conditions such as $y_p(x,\ 0)=0$ and $y_b(0)=1$ or $y_b(0)=0$

Because there exists an input and output stream in CSTR, σ is defined as $t_R D_e/R^2$, where t_R represents retention time of reactant in the reactor. When F is volumetric flow rate of reactant stream to the reactor, t_R can be obtained from V/F. Another parameter, β is defined as $\alpha k_0 E_0 t_R/S_0$, while z is 2, 1, or 0 for sphere, cylinder, and slab-type pellets. Thus, more parameters should be determined or modeling and analysis of CSTR, compared to simple batch-mode reactor. Usually, the pellets containing enzymes are assumed as empty particles that are free of reactant in initial stage of reaction, whereas the initial condition of bulk concentration can be chosen as $y_b(0)=1$ or $y_b(0)=0$.

At first, the transient response of CSTR was predicted by changing the size of spherical pellets from 0.0005 to 0.002 when $y_b(0)$ was assumed as 1. During continuous supply of input stream to reactor, abrupt addition of enzyme catalysts into the reactor was assumed at $\tau=0$. Though similar results have been obtained by other research groups, previous results are limited to only spherical pellets without inert core [19]. As summarized in Table 2, core-shell spherical pellets with x'=0.1 were assumed as catalytic particles for prediction of transient response of CSTR, by fixing k_0, K_e, K_m, Bi, α, and σ as 21, 5, 80, 10, 0.13333, and 0.72, respectively. Since the initial concentration of reactant in bulk medium was assumed as 1, the concentration decreased from 1 to its minimal value, followed by increasing of the concentration with increasing reaction time, as presented in Fig. 6(a). Because catalytic activity of the immobilized enzyme cannot be maintained permanently due to enzyme inactivation, the increase of reactant concentration was predicted after reaching its minimum value. Similar trend can be also expected regardless of enzyme inactivation, because the ability of enzymes

for conversion of reactant would be saturated due to continuous supply of reactant stream. Interestingly, the minimal value of reactant concentration decreased with decreasing size of the pellets, as displayed in Fig. 6(a). Because diffusion length inside the pellets decreases with decreasing value of R, the bulk concentration of reactant decreased as R decreased [29]. Similar trends were also observed from CSTR, when retention time, t_R, increased from 3,600 sec (σ=1.44) to 28,800 sec (σ=11.52), whereas the radius of spherical pellets was fixed as 0.0005 m. When t_R increases, the sufficient reaction time for treatment of reactant can be expected, causing decrease of minimal concentration, as shown in Fig. 6(b). In this article, the effect of the thickness of inert core was investigated in Fig. 6(c). When x' was close to 1 (x'=0.99), only slight decrease of reactant concentration was predicted, because enzymes are coated as thin skin layer on inert core, causing very weak catalytic effect. However, the minimal concentration decreased to a smaller value with decreasing value of x', because active volume of enzyme catalyst increases as a function of $1\text{-}x'^3$.

In this article, the transient responses of CSTR containing cylindrical and slab-type pellets were also studied by assuming the same reaction conditions adopted in Fig. 6(c), and the results are included in Fig. 7(a) and 7(b), respectively. Similar to core-shell spherical pellets, the conversion of reactant in the initial stage of reaction increased with decreasing value of x'. However, the minimal concentration of reactant was predicted as higher values than that of CSTR containing core-shell spherical pellets due to difference of particle geometry. Because the active volume of core-shell cylindrical and core-shell slab-type pellets with inert core is proportional to $1\text{-}x'^2$ and $1\text{-}x'$, respectively, a greater amount of enzymes can be included in the reactor containing core-shell spherical pellets under the same reaction conditions. Thus, the smallest minimal concentration of reactant was predicted from CSTR containing core-shell spherical pellets. As presented in Fig. 7(b), the transient behavior of CSTR containing slab-type pellets was more sensitive to x' compared to other types of pellets, indicating that core-shell

Table 2. Parameters for calculation of immobilized enzyme reactor (CSTR)

|	k_0	α	K_e	K_m	Bi	x'	β	σ	ω	Shape of pellets	Input	$y_b(0)$
Fig. 6(a)	21	0.13333	5	2	10	0.1	134.4	0.72	-	Core-shell sphere	Step	1
Fig. 6(b)	21	0.13333	5	2	10	0.6	134.4	VAR	-	Core-shell sphere	Step	1
Fig. 6(c)	21	0.13333	5	2	10	VAR	134.4	11.52	-	Core-shell sphere	Step	1
Fig. 6(d)	21	0.13333	0.002	2	10	0.1	134.4	11.52	-	VAR	Step	1
Fig. 7(a)	21	0.13333	5	2	10	VAR	134.4	11.52	-	Core-shell cylinder	Step	1
Fig. 7(b)	21	0.13333	5	2	10	VAR	134.4	11.52	-	Core-shell slab	Step	1
Fig. 7(c)	-	-	-	0.5	50	0.6	0.25	-	-	Core-shell sphere	Step	-
Fig. 8(a)	21	0.13333	80	2	10	0.1	VAR	VAR	-	Core-shell sphere	Step	0
Fig. 8(b)	21	0.13333	VAR	2	10	0.1	67.2	0.36	-	Core-shell sphere	Step	0
Fig. 8(c)	21	0.13333	80	2	10	VAR	168	0.9	-	Core-shell sphere	Step	0
Fig. 8(d)	21	0.13333	0.8	2	10	VAR	67.2	0.36	-	Core-shell sphere	Step	0
Fig. 9(a)	21	0.13333	0.8	2	10	VAR	67.2	0.36	-	Core-shell cylinder	Step	0
Fig. 9(b)	21	0.13333	0.8	2	10	VAR	67.2	0.36	-	Core-shell slab	Step	0
Fig. 10(a)	21	0.13333	80	2	10	0.1	VAR	VAR	-	Core-shell sphere	Pulse	0
Fig. 10(b)	21	0.13333	80	2	10	0.1	168	0.9	VAR	Core-shell sphere	Sinusoidal	0
Fig. 10(c)	21	0.13333	0	10000	10	0.001	16.8	1.44	-	Core-shell sphere	Step	0
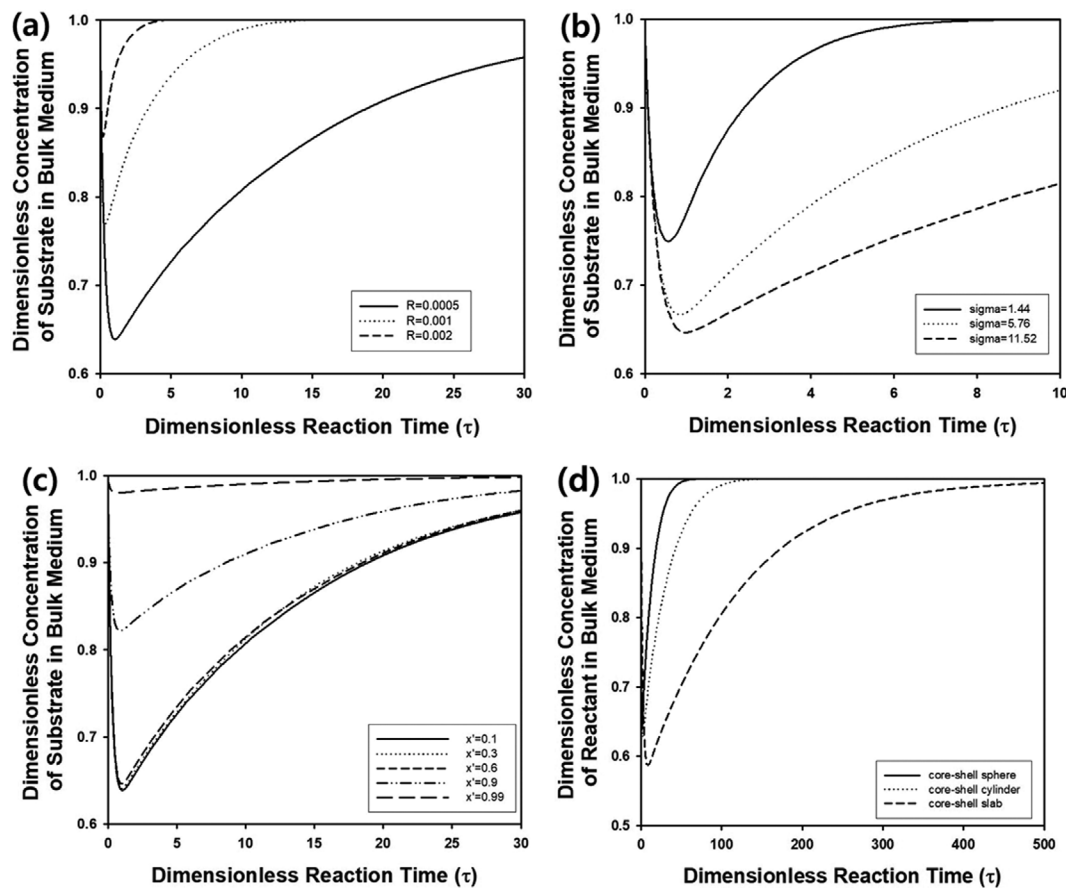
Fig. 6. (a) Change of the concentration of reactant in bulk fluid phase of CSTR containing core-shell spherical pellets as a function of reaction time for various values of the size of pellets. β, x′, σ, α, k$_0$, K$_e$, K$_m$, and Bi were fixed as 134.4, 0.1, 0.72, 0.13333, 21, 5, 2, and 10, respectively. (b) Change of the concentration of reactant in bulk fluid phase of CSTR containing core-shell spherical pellets as a function of reaction time for various values of σ. β, x′, α, k$_0$, K$_e$, K$_m$, and Bi were fixed as 134.4, 0.6, 0.13333, 21, 5, 2, and 10, respectively. (c) Change of the concentration of reactant in bulk fluid phase of CSTR containing core-shell spherical pellets as a function of reaction time for various values of x′. β, σ, α, k$_0$, K$_e$, K$_m$, and Bi were fixed as 134.4, 11.52, 0.13333, 21, 5, 2, and 10, respectively. (d) Change of the concentration of reactant in bulk fluid phase of CSTR containing core-shell pellets as a function of reaction time for three different types of the pellets. β, x′. σ, α, k$_0$, K$_e$, K$_m$, and Bi were fixed as 134.4, 0.1, 11.52, 0.13333, 21, 0.002, 2, and 10, respectively. y$_b$(0) was set to 1 and step input was assumed for all calculations.

spherical or cylindrical pellets are more advantageous for enzymatic reactions.

Reaction conversion at stationary state can be computed from Eq. (4) by assuming steady state ($\partial y_p/\partial\tau = \partial y_b/\partial\tau = 0$). In this case, the governing equations become nonlinear ODE, which can be also solved by finite element method using COMSOL. When β, Bi, and K$_m$ were 0.25, 50, and 0.5, respectively, Φ was adjusted from 0 to 10 to investigate the change of reaction conversion ($1-y_b$) at steady state for various values of x′ in core-shell spherical pellets. When x′ was 0, the results shown in Fig. 7(c) coincided well with previous results on spherical pellets without inert core computed by Lin using iterative Runge-Kutta method [30]. When x′ was close to 0, the conversion was maintained as similar value to that of a spherical pellet without inert core. When x′ was 0.6 and 0.9, the conversion decreased significantly due to the decrease of active volume with enzymes. For core-shell cylinder and slab with x′=0.6, similar trends were predicted, as included in the inset figure, which was obtained by assuming the same amount of the pellets (m$_p$).

The reaction conversion at steady state decreased in the order of sphere>cylinder>slab due to decrease of surface area of the pellets per unit volume of reactor.

When z equals to 2, 1, and 0, surface area of enzyme-immobilized pellets in unit volume of reactor can be represented as (z+1)/R(m$_p$/ρ_p)/V for spherical, cylindrical, and slab-type pellets in the reactor, respectively. Though the area decreases in the order of sphere>cylinder>slab for fixed value of the added mass and radius of the pellets, the same surface area can be assumed by adjusting R. For instance, 0.0005, 0.0003334, and 0.0001667 can be used as the radius for spherical, cylindrical, and slab-type pellets, respectively, to maintain the same surface area of the pellets. In this case, the Thiele modulus can be estimated as 9.3544, 6.2373, and 3.1187, respectively, whereas K$_e$ can be computed as 5, 2.2231, and 0.55578 for spherical, cylindrical, and slab-type pellets. Using these parameters, the change of reactant concentration in the exit stream of CSTR is plotted in Fig. 6(d) for three different types of pellets. Because K$_e$ of slab type particles was the smallest, the reactant concentration
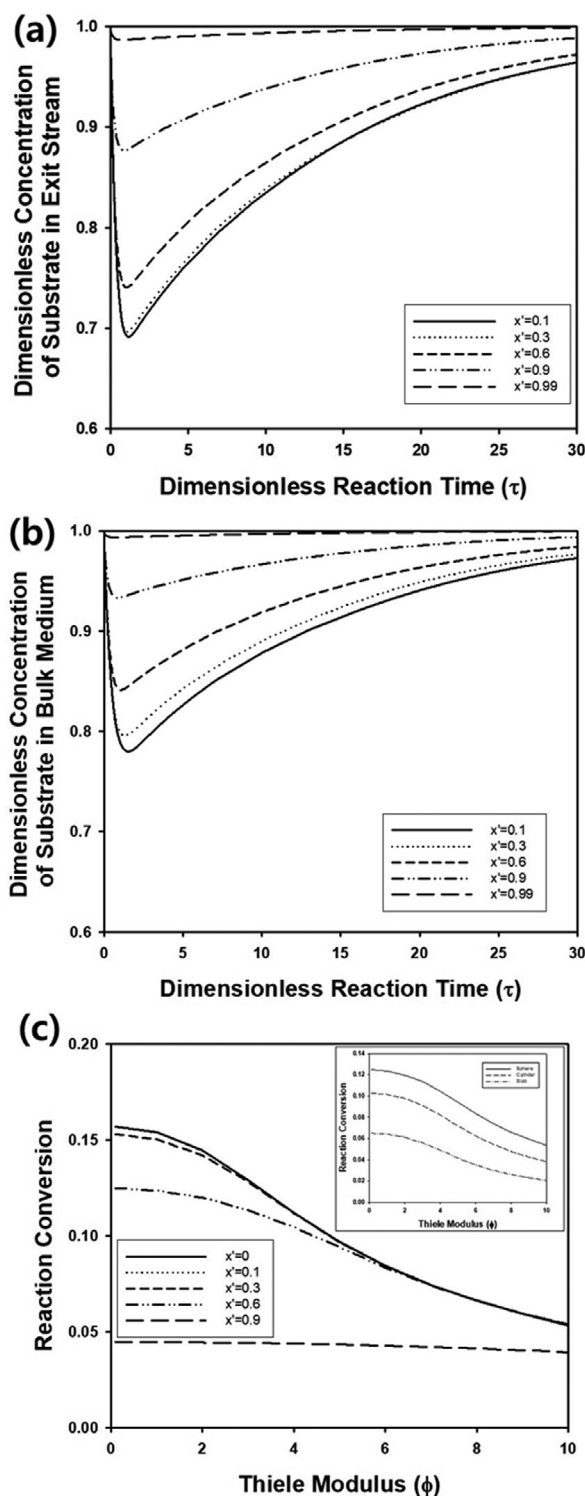
Fig. 7. Change of the concentration of reactant in bulk fluid phase of CSTR containing core-shell (a) cylindrical and (b) slab-type pellets as a function of reaction time for various values of x′. β, σ, α, k_0, K_e, K_m, and Bi were fixed as 134.4, 11.52, 0.13333, 21, 5, 2, and 10, respectively. $y_b(0)$ was set to 1 and step input was assumed for all calculations. (c) Change of steady-state concentration of substrate in fluid phase of CSTR containing core-shell spherical pellets. β, K_m, and Bi was fixed as 0.25, 0.5, and 50, respectively. Inset graph represents the results from core-shell cylindrical and slab-type pellets with x′=0.6.

increased as the most slowest manner, whereas the concentration in CSTR with spherical pellets increased most rapidly due to largest value of K_e.

In a CSTR, reactant-free immobilized enzymes can be included in the reactor before supplying reactant stream, assuming $y_b(0)=0$. When the concentration of reactant in input stream, $y_{in}(\tau)$, increases as a step function, the transient response of CSTR can be predicted by solving reaction-diffusion equations numerically, assuming nonlinear enzyme kinetics. Similar to the method adopted for Fig. 6, the effect of retention time on step response of CSTR containing core-shell spherical pellets was studied by changing the value of σ, as presented in Fig. 8(a). As σ increased with increasing value of retention time, the concentration of reactant in bulk medium increased slowly, because sufficient reaction time for removal of reactant can be expected with increasing retention time in CSTR. When σ was fixed as 0.36, the effect of enzyme inactivation was also studied by changing the inactivation parameter, K_e, as 0.08, 0.8, and 8, as shown in Fig. 8(b). For small value of K_e (0.08), the concentration increased from 0 and became saturated to about 0.5, followed by the second increasing period of the concentration as further reaction proceeded. However, the concentration increased consistently from 0 to 1 for larger value of K_e, implying that enzyme inactivation is not advantageous for removal of reactant in a continuous-mode reactor. In a batch reactor, a large value of K_e may result in delay of reaction time required to reach steady state and increase of the concentration at stationary state. In a CSTR under reactant-free initial condition, the effect of the thickness of inert core in core-shell spherical pellets was studied by fixing reaction parameters such as Bi, k_0, K_e, K_m, α, and σ as 10, 21, 80, 2, 0.13333, and 0.9. Though x′ was adjusted from 0.1 to 0.99, the transient responses of reactant concentration in bulk medium were predicted as similar values, as presented in Fig. 8(c). However, the effect of x′ became important, when σ decreased to 0.36, as displayed in Fig. 8(d), implying that a small value of x′ is more advantageous for removal of reactant under short retention time. As x′ increased, the increasing rate of the concentration in bulk medium became faster, implying that the active volume of pellets plays a significant role for removal of reactant.

In addition to spherical pellets, core-shell cylindrical and slab-type pellets were also considered as catalytic particles contained in an immobilized enzyme reactor as continuously stirred mode. Under the same reaction conditions adopted in Fig. 8(d), the results from core-shell cylindrical and slab-type pellets are included in Fig. 9(a) and 9(b), respectively. Similar to the results from core-shell spherical pellets, the concentration of reactant in bulk medium increased from 0 to 1 with increasing reaction time, and the increasing rate decreased with decreasing value of x′. However, the concentration in CSTR containing core-shell slab-type pellets increased more rapidly compared to the reactor having core-shell spherical and slab-type pellets due to the smallest surface area of the pellets per unit volume of the reactor among three types of pellets. Similar to a batch reactor, the bulk concentration depended more strongly on x′ compared to core-shell spherical or cylindrical pellets, as presented in Fig. 9(a) and 9(b).

In addition to step input, the application of pulse input to CSTR was also modeled by assuming core-shell spherical pellets (Fig.
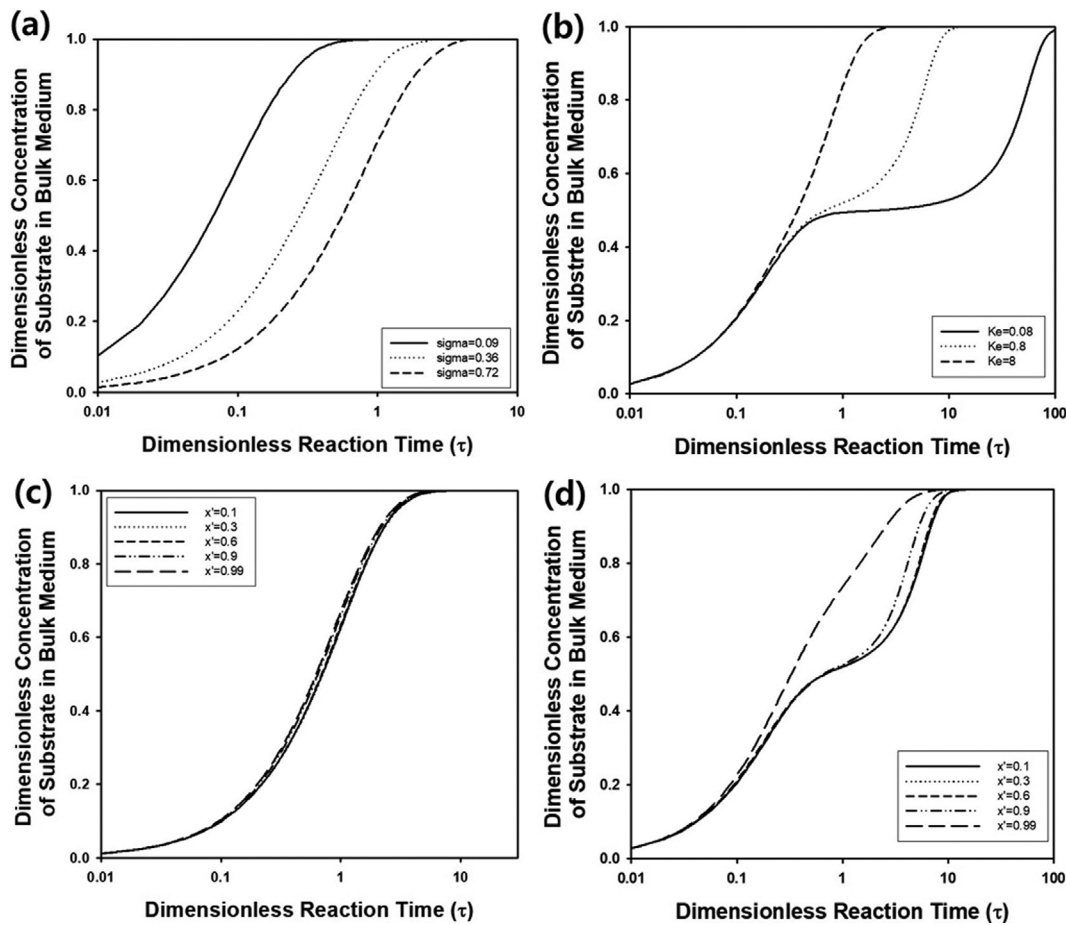
Fig. 8. (a) Change of the concentration of reactant in bulk fluid phase of CSTR containing core-shell spherical pellets for various values of σ. x′, α, k$_0$, K$_e$, K$_m$, and *Bi* were fixed as 0.1, 0.13333, 21, 80, 2, and 10, respectively. (b) Change of the concentration of reactant in bulk fluid phase of CSTR containing core-shell spherical pellets for various values of K$_e$. β, x′, σ, α, k$_0$, K$_m$, and *Bi* were fixed as 67.2, 0.1, 0.36, 0.13333, 21, 2, and 10, respectively. (c) Change of the concentration of reactant in bulk fluid phase of CSTR containing core-shell spherical pellets for various values of x′. β, σ, α, k$_0$, K$_m$, K$_e$, and *Bi* were fixed as 168, 0.9, 0.13333, 21, 2, 80, and 10, respectively. (d) Change of the concentration of reactant in bulk fluid phase of CSTR containing core-shell spherical pellets for various values of x′. β, σ, α, k$_0$, K$_m$, K$_e$, and *Bi* were fixed as 67.2, 0.36, 0.13333, 21, 2, 0.8, and 10, respectively. y$_b$(0) was set to 0 and step input was assumed for all calculations.

10(a)). Because enzyme inactivation was considered by setting K$_e$ as 80, the concentration of reactant in bulk medium increased from 0 to 1. At τ=0, step input was assumed, whereas Gaussian pulse with a standard deviation of 0.1 was applied at τ=0.3. As σ decreased, the influence of the pulse input became stronger, because short retention time resulted in less elimination of reactant from continuous input stream. However, only trace amount of pulse input can be observed for larger value of σ, causing consistent increasing transient response, which is similar to the response from step input. In Fig. 10(b), the effect of sinusoidal input was also investigated by predicting transient response of CSTR containing core-shell spherical pellets. During calculation, y$_{in}$(τ) was assumed as 1+Asin($\omega\tau$), in which A was set to 0.5, whereas ω was adjusted as 1, 5, and 10. As displayed in Fig. 10(b), the oscillation of response curve became more faster with increasing value of ω, though the concentration increased from 0 to larger value in overall, regardless of the value of ω.

In this study, the numerical solution obtained by COMSOL Multi-

physics was verified in an indirect manner, because analytical solutions involved in enzyme kinetics do not exist due to strong nonlinearity. Thus, K$_e$ was set to 0 and K$_m$ was assumed as very large value compared to y$_p$ from Eq. (4) to obtain the following linear coupled differential equations for approximate solution of immobilized enzyme reactor (CSTR).

$$\frac{\partial y_p}{\partial \tau} = \frac{1}{x^z}\frac{\partial}{\partial x}\left(x^z \frac{\partial y_p}{\partial x}\right) - \left(\frac{\phi^2}{K_m}\right)y_p$$

$$\text{and } \frac{dy_b}{d\tau} = \frac{1}{\sigma}[y_{in}(\tau) - y_b] - \left\{(z+1)\frac{\beta}{\sigma \cdot \phi^2}\right\}\left(\frac{\partial y_p}{\partial x}\right)_{x=1} \quad (5)$$

subject to boundary conditions such as $(\partial y_p/\partial r)_{x=x'}$=0 and $(\partial y_p/\partial x)_{x=1}$=Bi[y$_b$($\tau$)−y$_p$(1, τ)] and initial conditions such as y$_p$(x, 0)=0 and y$_b$(0)=1 or y$_b$(0)=0

The analytical solution of the above equation for core-shell spherical pellets (z=2) can be derived by Laplace transform, as the following result by Rosa et al. [31].
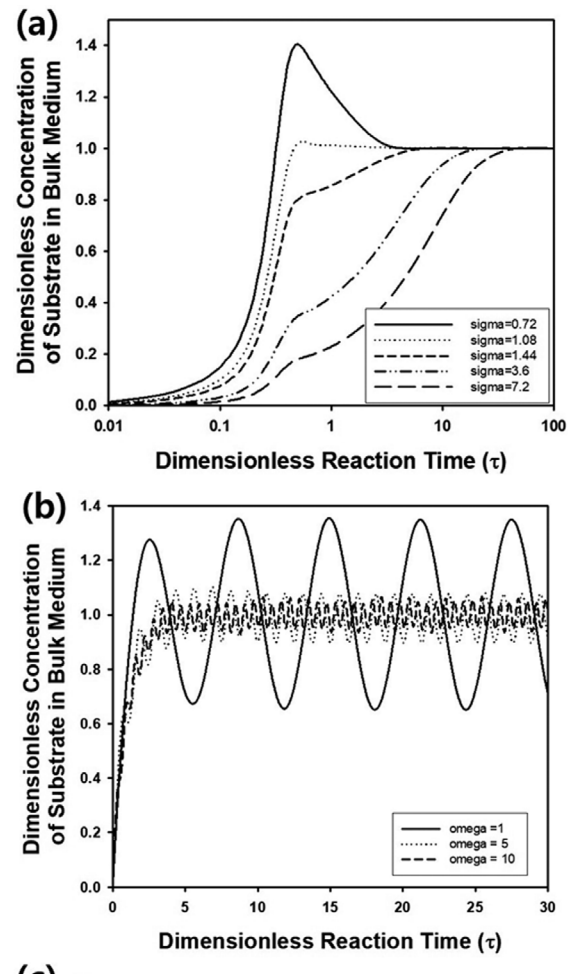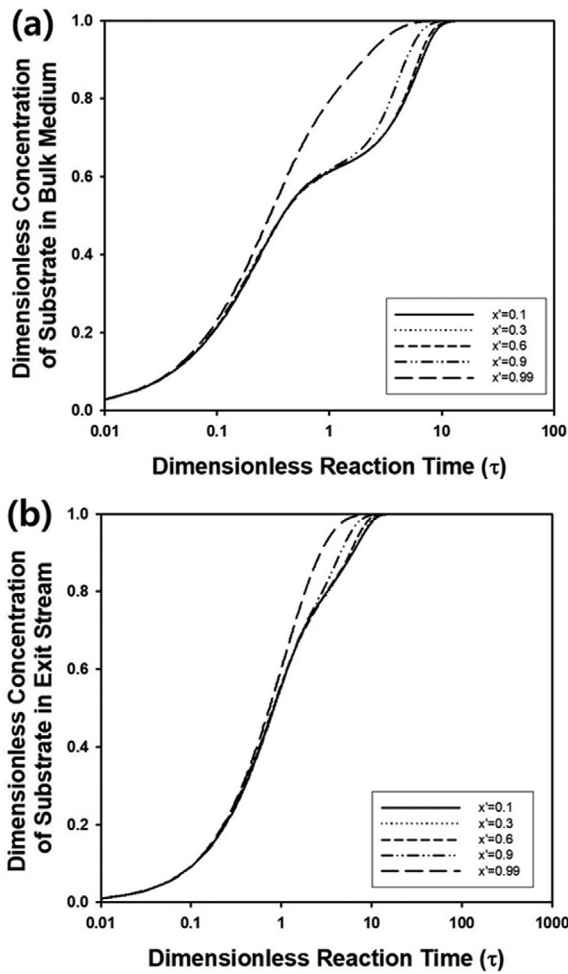
(a)

(b)

Fig. 9. Change of the concentration of reactant in bulk fluid phase of CSTR containing (a) core-shell cylindrical and (b) slab-type pellets for various values of x'. σ, α, k_0, K_m, K_e, and Bi were fixed as 0.36, 0.13333, 21, 2, 0.8, and 10, respectively. $y_b(0)$ was set to 0 and step input was assumed for all calculations.

$$y_b(\tau) = Bi\, \Psi_p \sum_{n=1}^{\infty} \frac{2(\xi_n^2 y_{b0} - A_n y_{p0}) \exp\{-(\xi_n^2 + \phi'^2)\tau\}}{D_n}$$

$$+ Bi\, \Psi_{in}\, \Psi_p \sum_{n=1}^{\infty} \frac{\dfrac{2\xi_n^2}{\xi_n^2 + \phi'^2}[1 - \exp\{-(\xi_n^2 + \phi'^2)\tau\}]}{D_n} \tag{6}$$

Here, Ψ_{in} is equal to $1/\sigma$, where Ψ_p and Φ' are $(z+1)\beta/(\sigma\Phi^2)$ and Φ^2/K_m, respectively. ξ_ns are eigenvalues satisfying the eigenvalue equations, $\xi_n(\Psi_p - A_n) = [\Psi_p + A_n(Bi-1)]\tan\xi_n$. D_n represents $(2\xi_n^2 + A_n Bi)$ $[\Psi_p + A_n(Bi-1)] + [\Psi_p - A_n + 2(Bi-1)](\Psi_p - A_n)\xi_n^2$, where A_n is defined as $\Phi^2 + \xi_n^2 - \Psi_{in}$. As shown in Table 3, the eigenvalues can be computed graphically using Desmos Graphic Calculator via the Internet, when Φ', Ψ_{in} and Ψ_p were fixed as 0.093541, 0.6944, and 1.2, respectively. Fig. 10(c) contains the change of the concentration of reactant in bulk medium predicted by the above approximate analytical solution and numerical result obtained using COMSOL Multiphysics. Because they coincide well with each other, the calculation results in this study can be trusted from the compared results in Fig. 10(c).

(a)

(b)

(c)

Fig. 10. (a) Change of the concentration of reactant in bulk fluid phase of CSTR containing core-shell spherical pellets for various values of σ. x', α, k_0, K_m, K_e, and Bi were fixed as 0.1, 0.13333, 21, 2, 80, and 10, respectively. $y_b(0)$ was set to 0 and pulse input was assumed for all calculations. (b) Change of the concentration of reactant in bulk fluid phase of CSTR containing core-shell spherical pellets for various values of ω. β, σ, x', α, k_0, K_m, K_e, and Bi were fixed as 168, 0.9, 0.1, 0.13333, 21, 2, 80, and 10, respectively. $y_b(0)$ was set to 0 and sinusoidal input was assumed for all calculations. (c) Comparison result of numerical and approximate analytical solution of CSTR for large value of K_e (K_e=10,000).

Table 3. Eigenvalues of approximate analytical solutions for large value of K_e (K_e=10,000)

ξ_1	ξ_2	ξ_3	ξ_4	ξ_5	ξ_6	ξ_7	ξ_8	ξ_9	ξ_{10}
0.815	2.882	5.735	8.667	11.658	14.69	17.75	20.829	23.923	27.026

3. Approximation of Fixed Bed Enzyme-immobilized Reactor by Connecting a Series of CSTRs

Because uniform concentration and temperature distribution can be expected under ideal mixing conditions, it is advantageous to use CSTRs for various reaction systems. However, fixed bed reactors are more practically used as immobilized enzyme reactors, since higher reaction conversion ad longer retention time can be expected, compared to other types of reactors. Due to mathematical complexity of the governing equations for fixed beds, the series connection of a sufficiently large number of CSTRs can be adopted as approximation of fixed beds, as applied to fixed bed adsorbers by Maria and Mansur [32]. With the aid of recent advances of the computer industry, the series connection of CSTRs can be modeled conveniently by COMSOL Multiphysics software. Because axial dispersion coefficient is an important feature in fixed bed reactors, the interchange of reaction products between connected CSTRs was modeled in the following manner, using interchange parameter, $\overline{\alpha}$.

$$\frac{\partial y_{p,i}}{\partial \tau} = \frac{1}{x^z}\frac{\partial}{\partial x}\left(x^z \frac{\partial y_{p,i}}{\partial x}\right) - \frac{\phi^2 \exp(-K_e\tau)y_{p,i}}{y_{p,i}+K_m} \quad (i=1,\dots,N)$$

$$\text{and } \sigma(1-\alpha)\frac{dy_{b,1}}{d\tau} = y_{in}(\tau)+\overline{\alpha}y_{b,2}-(1+\overline{\alpha})y_{b,1}-(z+1)\frac{\beta}{\phi^2}\left(\frac{\partial y_{p,1}}{\partial x}\right)_{x=1}$$

$$\sigma(1-\alpha)\frac{dy_{b,i}}{d\tau} = (1+\overline{\alpha})y_{b,i-1}+\overline{\alpha}y_{b,i+1}-\overline{\alpha}y_{b,i}-(1+\overline{\alpha})y_{b,i}$$

$$-(z+1)\frac{\beta}{\phi^2}\left(\frac{\partial y_{p,i}}{\partial x}\right)_{x=1} \quad (i=2,\dots,N-1)$$

$$\sigma(1-\alpha)\frac{dy_{b,N}}{d\tau} = (1+\overline{\alpha})y_{b,N-1}-\overline{\alpha}y_{b,N}-y_{b,N}-(z+1)\frac{\beta}{\phi^2}\left(\frac{\partial y_{p,N}}{\partial x}\right)_{x=1} \quad (7)$$

subject to boundary conditions such as $(\partial y_{p,i}/\partial r)_{x=x}$=0 and $(\partial y_{p,i}/\partial x)_{x=1}$=Bi$[y_{b,i}(\tau)-y_{p,i}(1,\tau)]$ and initial conditions such as $y_{p,i}(x,0)$=0 and $y_{b,1}(0)$=0

Here, σ is $t_{R,N}D/R^2$, where $t_{R,N}$ is defined as the retention time of ith CSTR. When total volume of N connected CSTRs is V, t_R, N
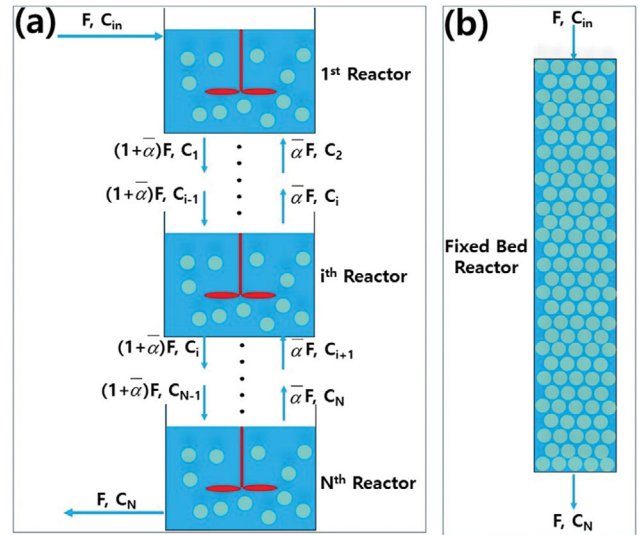
Fig. 11. (a) Schematic figure of cascade connection of CSTRs with interchanging streams between the connected reactors for approximation of (b) fixed bed reactors.

becomes V/(FN), which is smaller than the retention time mentioned in the previous section. Though axial dispersion in fixed bed reactor can be considered quantitatively using *Peclet* number (*Pe*), a new reaction parameter, $\overline{\alpha}$, was defined instead of *Pe* to specify the degree of material interchange between CSTRs connected in series, as presented in Fig. 11(a). In i^{th} CSTR, the dimensionless concentration of reactant inside pellets, $y_{p,i}$, and the concentration in bulk medium, $y_{b,i}$, can be computed by solving Eq. (5) simultaneously. Though the total number of differential equations is 2N, the concentration of reactant in exit stream from N^{th} CSTR can be considered as an approximate solution of the concentration at outlet stream of the fixed bed reactor shown in Fig. 11(b), if N is sufficiently large.

Table 4. Parameters for calculation of immobilized enzyme reactor (connected CSTRs). For all calculations, step input was applied, assuming $y_b(0)$=1

|	k_0	α	K_e	K_m	Bi	x'	β	σ	$\overline{\alpha}$	N	Shape of pellets
Fig. 12(a)	21	0.16667	0.08	2	10	0.1	VAR	0.0036	0.5	VAR	Core-shell sphere
Fig. 12(b)	21	0.7	0.08	2	10	0.1	7.056	0.00216	VAR	50	Core-shell sphere
Fig. 12(c)	21	VAR	0.08	2	10	0.1	3.024	0.00504	0	50	Core-shell sphere
Fig. 13(a)	21	0.7	0.08	2	100	VAR	7.056	0.00216	0.5	50	Core-shell sphere
Fig. 13(b)	21	0.7	0.08	2	VAR	0.6	7.056	0.00216	0.5	50	Core-shell sphere
Fig. 13(c)	21	0.7	0.08	2	10	0.1	VAR	VAR	0.5	50	Core-shell sphere
Fig. 14(a)	21	0.7	0.08	2	10	0.1	7.056	0.00216	0.5	50	VAR
Fig. 14(b)	21	0.7	0.08	2	10	0.1	7.056	0.00216	0	50	VAR
Fig. 14(c)	21	0.7	0.08	2	10	VAR	7.056	0.00216	0.5	50	VAR
Fig. 14(d)	0.21	0.7	0.08	2	10	VAR	7.056	0.00216	0.5	50	VAR
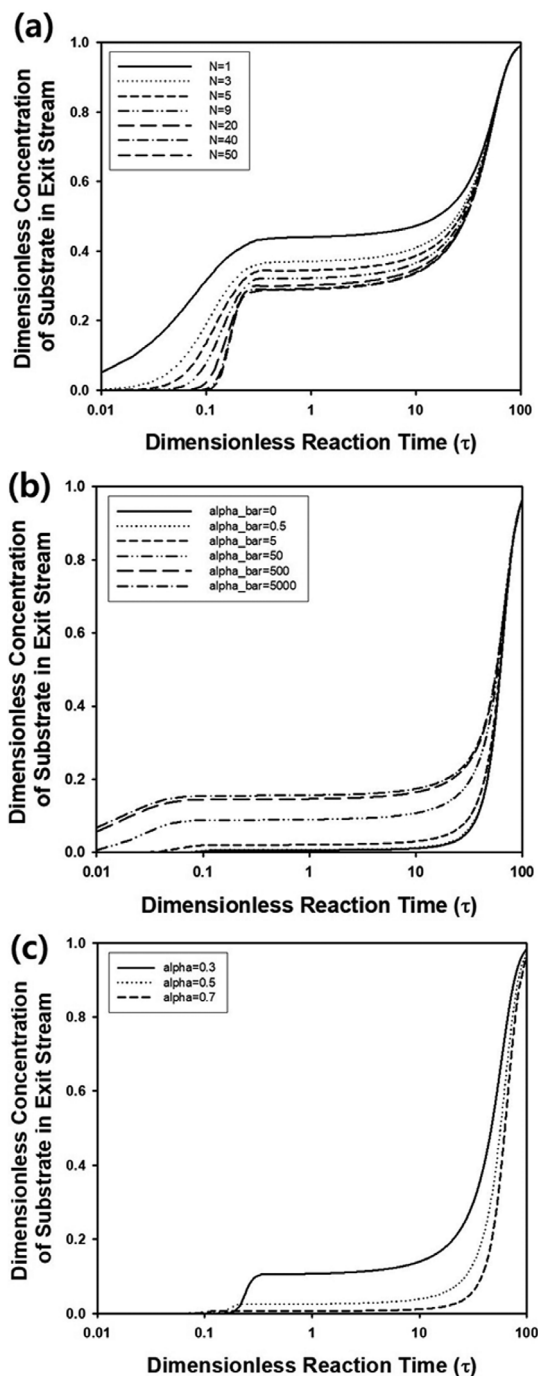
Fig. 12. (a) Change of the concentration of reactant in exit stream of connected CSTRs containing core-shell spherical pellets for various values of N. σ, x′, α, k_0, K_m, K_e, *Bi*, and $\overline{\alpha}$ were fixed as 0.0036, 0.1, 0.16667, 21, 2, 0.08, 10, and 0.5, respectively. **(b) Change of the concentration of reactant in exit stream of fixed bed reactor containing core-shell spherical pellets for various values of** $\overline{\alpha}$. β, σ, x′, α, k_0, K_m, K_e, and *Bi* were fixed as 7.056, 0.00216, 0.1, 0.7, 21, 2, 0.08, and 10, respectively. **(c) Change of the concentration of reactant in exit stream of fixed bed reactor containing core-shell spherical pellets for various values of** α. β, 0.1, 0.00504, 21, 2, 0.08, 10, and 0, respectively. $y_b(0)$ was set to 0 and step input was assumed for all calculations.

To determine the proper number of CSTRs, N, reaction parameters such as *Bi*, x′, k_0, K_e, K_m, α, and $\overline{\alpha}$ were fixed as 10, 0.1, 21, 0.08, 2, 0.13333, and 0.5, respectively, as summarized in Table 4. Then, transient responses were compared by changing N from 1 to 50, assuming step input to the first reactor. As presented in Fig. 12(a), the transient response of the exit stream in connected reactors converged to the result from N=50, and the reactor performance was improved by connecting CSTRs in series. Thus, N was fixed as 50 for an approximation of a fixed bed reactor. For further calculations, α was set to 0.7, because the packing fraction of close packed spherical immobilized-enzyme pellets can be increased to 0.74. To study the effect of dispersion in packed bed reactors, $\overline{\alpha}$ was adjusted from 0 to 5000, and the results are plotted in Fig. 12(b). When there was no axial dispersion ($\overline{\alpha}=0$), the concentration of reactant in exit stream was predicted as slightly larger value than 0, followed by gradual increase up to 1 due to inactivation of enzyme. As $\overline{\alpha}$ increased, the concentration increased rapidly and reached a plateau value until τ became about 10, followed by the second period of the concentration rising. Because the behavior of connected CSTRs with larger value of $\overline{\alpha}$ can be considered as one CSTR with perfect mixing, relatively higher concentration in the response curve was predicted from $\overline{\alpha}=5,000$, as presented in Fig. 12(b). In Fig. 12(c), the effect of catalyst loading on the performance of the fixed bed reactor was investigated by changing α as 0.3, 0.5, and 0.7, when N was fixed as 50. When α was relatively small ($\alpha=$ .3), the concentration in the exit stream increased to about 0.13, followed by abrupt rise of the concentration up to 1 due to insufficient enzyme loading and inactivation of enzymes. However, the concentration was maintained as a quite small value close to 0, followed by increase up to 1 due to enzyme inactivation when α was large ($\alpha=0.7$).

The effect of inert core thickness of core-shell enzyme-immobilized pellets was also studied by approximating a fixed bed reactor as N CSTRs connected in series. For core-shell spherical pellets, x′ was adjusted from 0.1 to 0.99, while α and $\overline{\alpha}$ were fixed as 0.7 and 0.5, respectively, and the response curves were predicted by assuming a step input, as presented in Fig. 13(a). Though the concentration increased from 0 to 1 for all cases, the increasing rate of the concentration decreased with decreasing value of x′, indicating that the reactor performance can be enhanced by increasing the active volume of enzyme catalyst in the core-shell pellets. In Fig. 13(b), the effect of *Biot* number was investigated by fixing x′ and α as 0.6 and 0.5, respectively. When *Bi* was small (*Bi*=0.1), the concentration increased rapidly in the initial stage of operation time, because the mass flux from bulk medium to the pellets decreased due to increased mass transfer resistance in surrounding films on the pellets. When *Bi* was sufficiently large (*Bi*=100), the concentration of exit stream was kept as a small value close to 0 until $\tau=10$, followed by abrupt rise of the concentration up to 1 due enzyme inactivation, as presented in Fig. 13(b). The effect of retention time, t_R, was investigated in Fig. 13(c) by changing t_R from 28.8, 288, and 2,880. Similar to a simple CSTR, the concentration of reactant in the exit stream increased rapidly for small value of t_R, whereas the concentration increased as a slow rate for sufficiently large value of t_R.

In addition to spherical pellets, cylindrical and slab-type catalysts were also considered as immobilized enzyme pellets in fixed
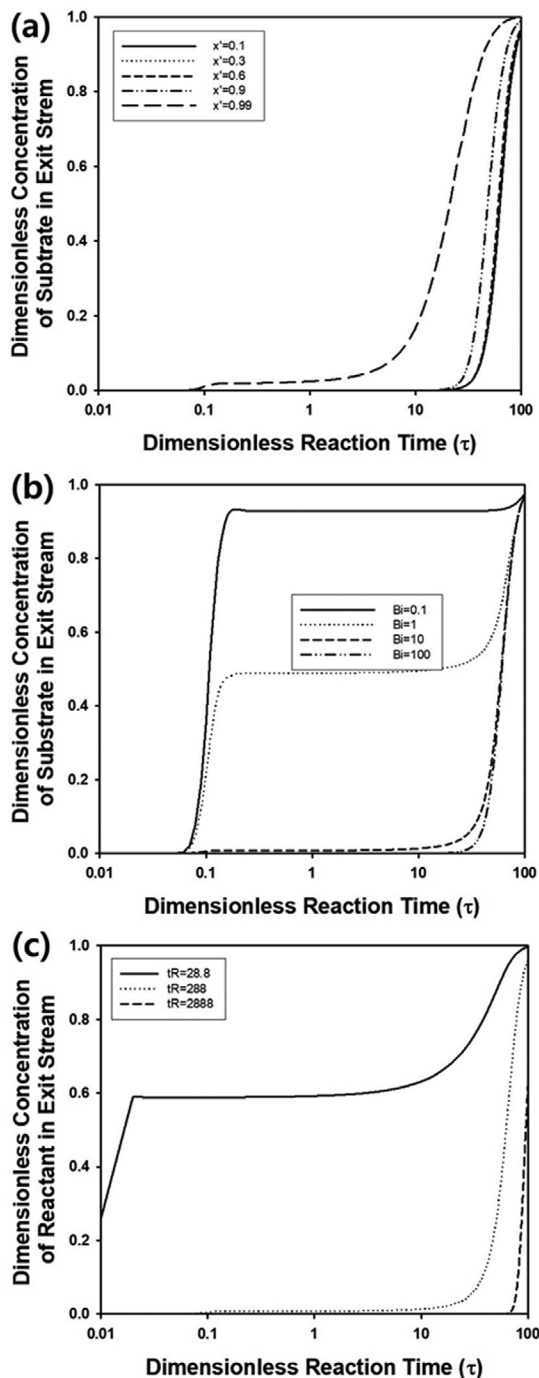
Fig. 13. (a) Change of the concentration of reactant in exit stream of fixed bed reactor containing core-shell spherical pellets for various values of x′. β, σ, α, k_0, K_m, K_e, *Bi*, and $\overline{\alpha}$ were fixed as 7.056, 0.00216, 0.7, 21, 2, 0.08, 100, and 0.5, respectively. (b) Change of the concentration of reactant in exit stream of fixed bed reactor containing core-shell spherical pellets for various values of *Bi*. β, x′, σ, α, k_0, K_m, K_e, and $\overline{\alpha}$ were fixed as 7.056, 0.6, 0.00216, 0.7, 21, 2, 0.08, and 0.5, respectively. (c) Change of the concentration of reactant in exit stream of fixed bed reactor containing core-shell spherical pellets for various values of retention time. x′, α, k_0, K_m, K_e, *Bi*, and $\overline{\alpha}$ were fixed as 0.1, 0.7, 21, 2, 0.08, 10, and 0.5, respectively. $y_b(0)$ was set to 0 and step input was assumed for all calculations.

bed reactor. As presented in Fig. 14(a), the change of reactant concentration in exit stream increased with increasing reaction time, when K_e and k_0 was set to 0.08 and 21, respectively, to account for enzyme inactivation. The most rapid increasing rate of the concentration in fixed bed reactor containing slab-type pellets was predicted, because the surface area per unit volume of the reactor decreased in the order of sphere>cylinder>slab. As displayed in Fig. 14(b), similar trends were predicted from breakthrough curves, when there was no enzyme inactivation (K_e=0). Unlike the results with enzyme inactivation, the concentration at stationary state was observed for the fixed bed reactor containing each pellet, since the rate constant is independent of reaction time. When enzyme inactivation was not assumed, the effect of the thickness of inert core was investigated for each type of pellet. Fig. 14(c) contains the change of the steady-state concentration and reaction conversion of fixed bed reactor, when k_0 was fixed as 21. Because the Thiele modulus was assumed as a large value (Φ=37.417), the concentration at stationary state was kept as almost constant value, when x′ was smaller than 0.9. However, the steady-state concentration increased drastically regardless of the shape of the pellet, when x′ became larger than 0.9 due to incomplete active volume of the biocatalyst, while the reaction conversion showed a reverse trend. In Fig. 14(c), the Thiele modulus was assumed as 37.417 by setting k_0, R, D, E_0, and S_0 as 21 M/s, 0.0005 m, 10^{-10} m²/s, 5×10^{-6} M, and 3×10^{-3} M, respectively. E_0 and S_0 were adopted as the same value suggested by Lin for enzyme pellets without core [19]. Because they adopted 0.05 to 0.1 cm for R, 0.5 mm was chosen in Fig. 14(c). Thus, k_0 was assumed as 21 to obtain Φ=37.417, which is comparable to the value of Φ adopted in previous research by Lin et al. (Φ=50 or 2 to 10). As presented in Fig. 14(d), the steady-state concentration increased consistently with increasing value of x′, when k_0 decreased to 0.21 (Φ=3.7417). The conversion decreased from initial value to 0 gradually increasing value of x′, indicating that the shell of the core-shell pellets should be sufficiently thick to ensure the high conversion under the reaction condition of low rate constant.

CONCLUSIONS

Mathematical modeling of three kinds of immobilized enzyme reactors--batch, CSTR, and fixed bed reactor--was carried out by assuming Michaelis-Menten kinetics with time-dependent rate constant to take into account enzyme inactivation. After the coupled governing equations were solved by finite element method, the concentration in bulk fluid phase and intra-particle concentration inside the immobilized enzyme pellets could be calculated for the reactors containing spherical, cylindrical, and slab-type pellets and their core-shell particles. In batch-mode reactor with finite volume, the decreasing rate of the reactant concentration in bulk medium increased with increasing value of *Biot* number due to decrease of mass transfer resistance in the film surrounding the pellets. Regardless of the shape of the pellets, the steady-state concentration in batch reactor decreased with increasing value of catalyst loading and Thiele modulus due to enhanced catalytic effect, whereas the concentration increased with increasing value of inert-core thickness due to decrease of active volume of the pellets. The intra-particle concentration could be also computed for various shapes of the pellets,
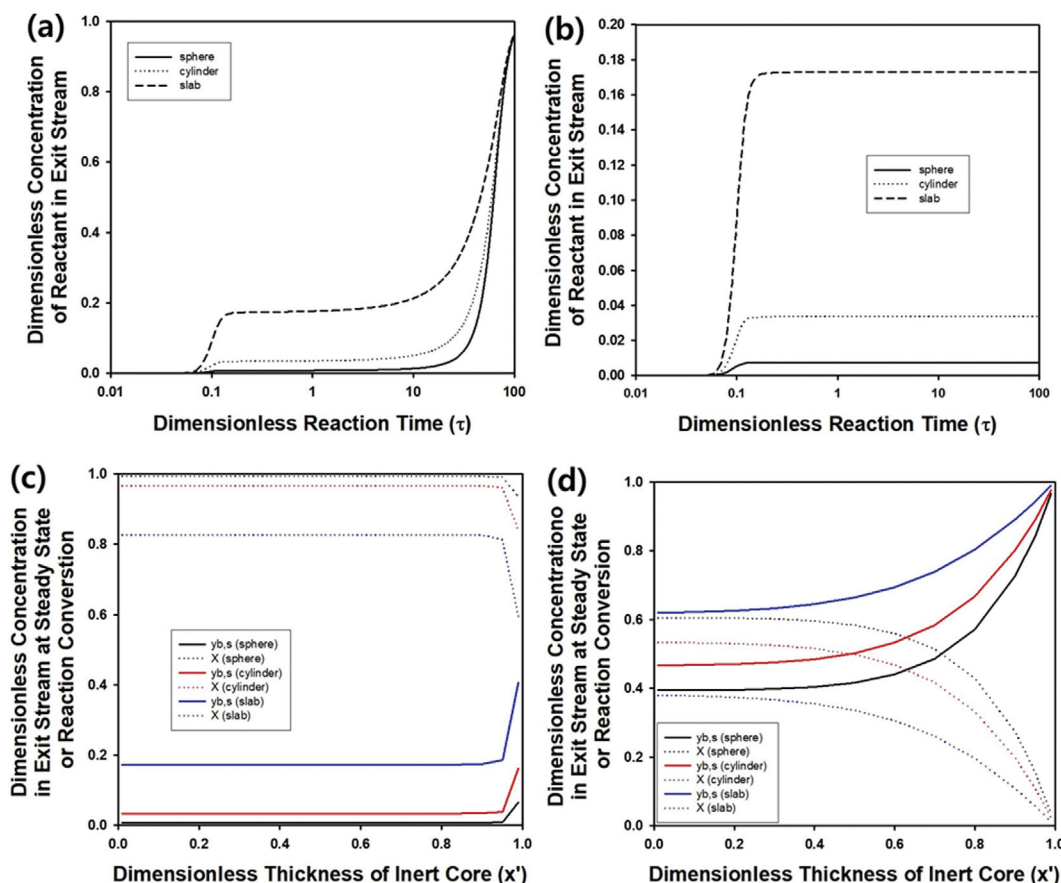
Fig. 14. (a) Change of the concentration of reactant in exit stream of fixed bed reactor containing core-shell spherical, cylindrical, and slab-type pellets. β, x′, σ, α, k_0, K_m, K_e, *Bi*, and $\overline{\alpha}$ were fixed as 7.056, 0.1, 0.00216, 0.7, 21, 2, 0.08, 10, and 0.5, respectively. (b) Change of the concentration of reactant in exit stream of fixed bed reactor containing core-shell spherical, cylindrical, and slab-type pellets. β, x′, σ, α, k_0, K_m, K_e, *Bi*, and $\overline{\alpha}$ were fixed as 7.056, 0.1, 0.00216, 0.7, 21, 2, 0.08, 10, and 0, respectively. $y_b(0)$ was set to 0 and step input was assumed for all calculations. (c) and (d) Change of the steady-state concentration and conversion of reactant in exit stream of fixed bed reactor containing core-shell spherical, cylindrical, and slab-type pellets for various values of x′. 7.056, β, σ, α, K_m, K_e, *Bi*, and $\overline{\alpha}$ were fixed as 0.00216, 0.7, 21, 2, 0.08, 10, and 0.5, respectively. k_0 was assumed as 21 and 0.21 for (c) and (d), respectively.

which showed that time evolution of the concentration profile led to uniform distribution of the reactant concentration after sufficient reaction time.

In a continuous reactor like the CSTR, the concentration in bulk phase increased gradually due to enzyme inactivation, when there was no reactant in the reactor before start-up. The retention time was found to be an important parameter to control the concentration in bulk phase of CSTR, because the concentration increased more rapidly with increasing feed flow rate due to insufficient retention time for complete removal of reactant. When the reactant was contained in the reactor initially, the concentration in bulk medium decreased to its minimal value, finally increasing to initial concentration due to inactivation of the enzymes. The minimum concentration was dependent on various reaction parameters such as the size of the pellets, feed flow rate, and the thickness of inert core as well as the shape of the pellets.

Fixed bed reactors were approximated by assuming the cascade connection of sufficient number of CSTRs, assuming exchange of reactant and product between the connected CSTRs. When enzyme inactivation became serious with increasing reaction time, the approximation results showed that the increasing trend of the concentration in the exit stream resembled the breakthrough curve of fixed bed adsorbers, When no enzyme inactivation was assumed, the concentration reached stationary-state values, which decreased in the order of slab>cylinder>sphere due to surface area of the pellets per unit volume of the reactor. Similar to a simple CSTR, the increasing rate of the concentration decreased with increasing amount of catalyst loading, the shell thickness of the pellets, *Biot* number, and retention time. Similar to batch reactors, the reaction conversion increased with decreasing value of inert core thickness, x′, because more reactant can be treated by the pellets with thick shell with enzymatic activity.

The modeling concept of core-shell enzyme catalyst with inert core in this study is advantageous in that practical application of enzymes has been developed by immobilization of enzymes onto glass beads as core material. Practically, the regeneration and repeated uses of enzyme-immobilized beads are crucial for stable operation of biochemical processes, which can be modeled by using the core-shell structured particles in this study in a more realistic manner.

REFERENCES

1. S. Datta, L. R. Christena and Y. R. S. Rajaram, 3 *Biotech*, **3**, 1 (2013).
2. A. Basso and S. Serban, *Mol. Catal.*, **479**, 110607 (2019).
3. A. S. Simões, L. Ramos, L. Freitas, J. C. Santos, G. M. Zanin and H. F. de Castro, *Biofuel Res. J.*, **6**, 242 (2015).
4. B. Wouters, S. A. Currivan, N. Abdulhussain, T. Hankemeier and P. J. Schoenmakers, *Trends Anal. Chem.*, **144**, 116419 (2021).
5. C. B. Ching and K. H. Chu, *Appl. Microbiol. Biotechnol.*, **29**, 316 (1988).
6. I. M. Abu-Reesh, *Bioprocess Eng.*, **17**, 131 (1997).
7. A. Illanes, L. Wilson and L. Raiman, *Bioprocess Eng.*, **21**, 509 (1999).
8. J. G. Palencia and E. M. Verruschi, *Chem. Eng. Trans.*, **27**, 379 (2012).
9. A. Ghadi, F. Tabandeh, S. Mahjoub, A. Mohsenifar, F. T. Roshan and R. S. Alavije, *J. Oleo Sci.*, **64**(4), 423 (2015).
10. L. Li, Z. Gao, H. Zhang, H. Du, C. Ren, S. Qi and H. Chen, *New J. Chem.*, **45**, 11153 (2021).
11. R. Varshney, S. Sharma, B. Prakash, J. K. Laha and D. Patra, *ACS Omega*, **4**, 13790 (2021).
12. Z. Gan, T. Zhang, Y. Liu and D. Wu, *Plos One*, **7**(10), e47154 (2012).
13. M. Moo-Young and T. Kobayashi, *Can. J. Chem. Eng.*, **50**, 162 (1972).
14. N. E. Moreira and F. X. Malcata, *J. Chem. Eng. Jpn.*, **29**(2), 392 (1996).
15. V. Bales and P. Rajniak, *Chem. Papers*, **40**(3), 329 (1986).
16. A. E. AL-Muftaha and I. M. Abu-Reesh, *Biochem. Eng. J.*, **23**, 139 (2005).
17. P. Valencia, S. Flores, L. Wilsona and A. Illanes, *Biochem. Eng. J.*, **49**, 256 (2010).
18. R. Fraas and M. Franzreb, *Biocatal. Biotransfor.*, **35**(5), 337 (2017).
19. S. H. Lin and C. K. Wei, *Chem. Eng. Sci.*, **34**, 827 (1979).
20. S. Hertzberg, L. Kvittingen, T. Anthonsen and G. Skjåk-Braek, *Enzyme Microb. Technol.*, **14**(1), 42 (1992).
21. G. Xiu, L. Jiang and P. Li, *Ind. Eng. Chem. Res.*, **39**(11), 4054 (2000).
22. S. H. Lin, *Biophys. Chem.*, **8**, 105 (1978).
23. P. De Santis, L.-E. Meyer and S. Kara, *React. Chem. Eng.*, **5**, 2155 (2020).
24. A. Sanchez, J. Cruz, N. Rueda, J. C. S. dos Santos, R. Torres, C. Ortiz, R. Villalonga and R. Fernandez-Lafuente, *RSC Adv.*, **6**, 27329 (2016).
25. G. Pettersson, *Eur. J. Biochem.*, **69**, 273 (1976).
26. Y. Hayashi, S. Santoro, Y. Azuma, F. Himo, T. Ohshima and K. Mashima, *J. Am. Chem. Soc.*, **135**, 6192 (2013).
27. Y.-S. Cho and S. Sung, *Korean J. Chem. Eng.*, **37**(11), 1836 (2020).
28. U. Mehmetoglu, *Enzyme Microb. Technol.*, **12**, 124 (1990).
29. P. Li, G. Xiu and A. E. Rodrigues, *Chem. Eng. Sci.*, **58**, 3361 (2003).
30. S. H. Lin, *J. Appl. Chem. Biotechnol.*, **28**, 677 (1978).
31. J. O. M. Rosa, R. M. Escobar, T. V. Garcia and J. A. Ochoa-Tapia, *Chem. Eng. Sci.*, **57**, 1409 (2002).
32. M. E. Maria and M. B. Mansur, *Braz. J. Chem. Eng.*, **34**(3), 901 (2017).